Published online 22 October 2011 *Nucleic Acids Research, 2012, Vol. 40, No. 4* ***1787–1796***
doi:10.1093/nar/gkr864

Quality control of *MAT*a1 splicing and exon skipping by nuclear RNA degradation

Defne E. Egecioglu, Tadashi R. Kawashima and Guillaume F. Chanfreau*

Department of Chemistry & Biochemistry and the Molecular Biology Institute, University of California, Los Angeles CA 90095-1569, USA

Received July 7, 2011; Revised September 26, 2011; Accepted September 27, 2011

ABSTRACT

The *MAT*a1 gene encodes a transcriptional repressor that is an important modulator of sex-specific gene expression in *Saccharomyces cerevisiae*. *MAT*a1 contains two small introns, both of which need to be accurately excised for proper expression of a functional *MAT*a1 product and to avoid production of aberrant forms of the repressor. Here, we show that unspliced and partially spliced forms of the *MAT*a1 mRNA are degraded by the nuclear exonuclease Rat1p, the nuclear exosome and by the nuclear RNase III endonuclease Rnt1p to prevent undesired expression of non-functional a1 proteins. In addition, we show that mis-spliced forms of *MAT*a1 in which the splicing machinery has skipped exon2 and generated exon1–exon3 products are degraded by the nuclear 5′–3′ exonuclease Rat1p and by the nuclear exosome. This function for Rat1p and the nuclear exosome in the degradation of exon-skipped products is also observed for three other genes that contain two introns (*DYN2*, *SUS1*, *YOS1*), identifying a novel nuclear quality control pathway for aberrantly spliced RNAs that have skipped exons.

INTRODUCTION

The protein product of the *MAT*a1 gene in *Saccharomyces cerevisiae*, also called 'a1', is a transcriptional regulator, and, together with the alpha2 protein, specifically acts to repress the expression of haploid-specific genes as well as the HO gene in wild-type diploid cells (1). Both of these proteins are also normally expressed in their respective haploid cells, under the haploid-specific transcriptional program for either *MAT*a or MATalpha cells (Figure 1A). *MAT*a1 has not been shown to have a specific function in haploid *MAT*a cells (although it is expressed constitutively), but is thought to play a role in the expression of mating pheromones (2). On the other hand, alpha2 represses *MAT*a-specific gene expression in MATα cells. In the case of diploid cells, these two homeodomain containing proteins heterodimerize and bind DNA cooperatively in order to repress the haploid-specific transcriptional program (3). *MAT*a1 contains a homeodomain region between residues 66 and 126, which is important for a1 biological function. Structural studies have shown that within the a1 protein, Helices 1 and 2 of the homeodomain are important for maintaining contact with alpha2, whereas Helix 3 is important for mediating interactions with DNA (4). While a1 alone does not display any sequence specific DNA binding properties, the a1-alpha2 heterodimer has 3000-fold increase in sequence recognition when compared to alpha2 alone (5,6).

The gene encoding *MAT*a1 is unusual, as it is one of the few *S. cerevisiae* genes containing two introns (7–9) (Figure 1A). In addition, these introns are smaller than most *S. cerevisiae* introns. Because exon3 is also small, previous studies have shown that partially spliced *MAT*a1 mRNAs that have excised intron 1 but retain intron2 have the potential to encode a protein which is actually longer than the wild-type version and is inactive (8). Thus, it is important that the splicing of *MAT*a1 occurs accurately, in order to prevent the accumulation of unspliced or partially spliced forms that would be non-functional. In this study, we show that unspliced and partially spliced forms of *MAT*a1 are degraded by nuclear RNA turnover pathways. In addition, we demonstrate the existence of a novel RNA degradation mechanism that specifically targets exon2 skipped products of *MAT*a1 and of three other genes that contain two introns (*DYN2*, *SUS1*, *YOS1*). These studies show that

*To whom correspondence should be addressed. Tel: +1 310 825 4399; Fax: +1 310 206 4038; Email: guillom@chem.ucla.edu
Present address:
Defne E. Egecioglu, Department of Molecular Biosciences, Northwestern University. Evanston, IL 60208, USA.

The authors wish it to be known that, in their opinion, the first two authors should be regarded as joint First Authors.

© The Author(s) 2011. Published by Oxford University Press.
This is an Open Access article distributed under the terms of the Creative Commons Attribution Non-Commercial License (http://creativecommons.org/licenses/by-nc/3.0), which permits unrestricted non-commercial use, distribution, and reproduction in any medium, provided the original work is properly cited.

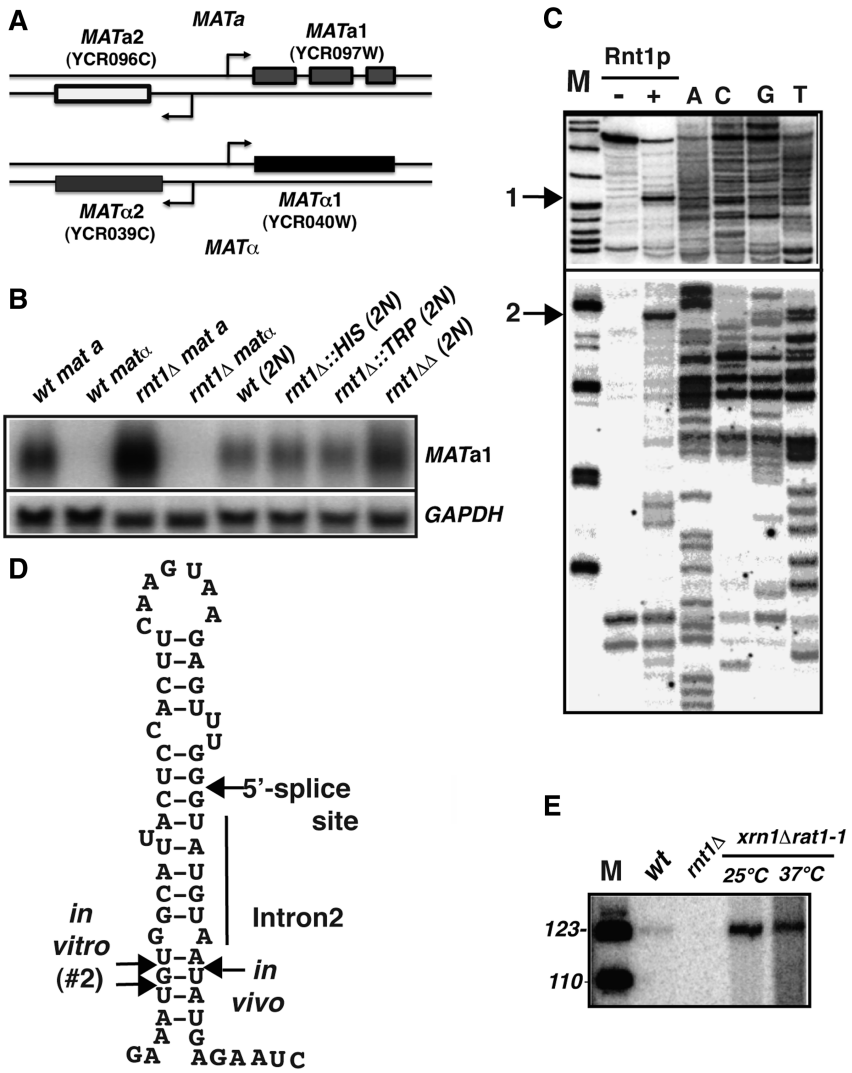

Figure 1. Architecture of the *MAT* locus, analysis of *MAT*a1 expression in Rnt1p mutant strains and cleavage by Rnt1p. **(A)** Schematic representation of gene structures at the *MAT*a and *MAT*alpha loci. **(B)** Northern blot analysis of *MAT*a1 expression in wild-type and *rnt1Δ* strains in the SK1 background. 2N indicate diploid cells. **(C)** *In vitro* cleavage of a model *MAT*a1 substrate by recombinant Rnt1p. Shown is a primer extension analysis of RNAs incubated in buffer or with recombinant Rnt1p. A sequencing ladder was obtained using the same oligonucleotide. 1 and 2 indicate the location of the major cleavage products. No other cleavage products were observed in the central portion of the gel which is not shown. **(D)** Predicted Rnt1p stem–loop structure. Shown are the locations of the cleavage sites mapped *in vitro* (panel C) or *in vivo* (panel E). **(E)** RT–PCR analysis of Rnt1p cleavage intermediates. RNAs presenting a 5′-phosphate group from the corresponding strains were ligated to an adaptor RNA, amplified using a *MAT*a1-specific reverse primer and an adaptor forward primer, and fractionated on an acrylamide gel.

the splicing of *MAT*a1 is relatively inefficient, and that nuclear degradation mechanisms have evolved to limit the accumulation of mRNAs that have escaped the splicing machinery or that have been aberrantly spliced.

MATERIALS AND METHODS

Yeast strains and media

Strains of mating type-a (*MAT*a) were utilized, unless otherwise indicated. Yeast strains were grown at 30°C until mid-log phase (OD600 = 0.4–0.6), in YPD medium unless indicated otherwise. The majority of the strains used in this study were in the BMA64 (10) or BY4741 (Open Biosystems) backgrounds and were described previously (11,12). The SK1 (13) derived strains used in this study were:

KBY257 (n) MATa, wild-type; KBY258 (n) MATα, wild-type; KBY257 (n) *rnt1::HIS*; KBY258 (n) *rnt1::TRP*; KBY (2n) *rnt1::HIS*, *RNT1*; KBY (2n) *rnt1::TRP*, *RNT1*; KBY (2n) *RNT1*, *RNT1*; KBY (2n) *rnt1::HIS* r*nt1::TRP*. SK1 strains were grown in 30°C at steady state. The *xrn1Δ*::*URA rat1-1* (MATa) strain was obtained from the Tollervey Lab (14), and was grown at 25°C until mid-log phase, and then shifted to 37°C for 3 h utilizing pre-warmed media. For generation of the *rnt1*::*KAN* replacement in the *xrn1Δ rat1-1* strain, PCR-based disruption of the *RNT1* gene was performed as described in Longtine *et al.* (15) through the amplification of the KAN^R marker.

RNA analysis

The list of oligonucleotides used in this study is provided in Supplementary Table S1. Templates for *in vitro* RNA transcription were obtained through PCR amplification of *MAT*a1 sequences and incorporating a T3 RNA Polymerase promoter sequence at their 5′-ends. *In vitro* transcription was performed using the T3 MEGAScript or MAXIScript kits (Applied Biosystems/Ambion), and the resulting RNAs were purified through phenol::chloroform extraction, and checked on both native and denaturing gels prior to further experimentation. *In vitro* cleavage assays with purified recombinant His6-Rnt1p were carried out generally as described (16). Primer extension on cleaved *in vitro* transcribed RNAs for mapping cleavage sites was performed as described (16).

Total RNA extraction from yeast under denaturing conditions and subsequent northern blotting analysis were performed as described (16). Detection of RNA species on northern blots was performed using either 5′-labeled oligonucleotides, PCR probes, or riboprobes. Riboprobes were generated using the T3 MAXI kit (Applied Biosciences/Ambion) and hybridized to membranes as described (17).

Primer extension on total RNAs was performed as in (11,18) using 5–10 μg of denatured total RNA. The various primers used for reverse transcription and PCR amplification are listed in Supplementary Table S1. An amount of 40 μg of total RNA were digested with Ambion RNase-free Turbo DNase (8 U enzyme) for 45 min at 37°C in 200 μl. The reaction was phenol–chloroform extracted with equal volume organic and ethanol-precipitated. The digested RNA was then resuspended in 20 μl water and quantitated. An amount of 5 μg of DNase treated RNA was combined with 0.4 μl (25 mM each) dNTPs and 1 μl of 50 ng/μl random primer mix to a total volume of 12 μl. The mixture was heated to 65°C for 5 min, followed by placing on ice for 2 min. This cooled mixture was combined with Invitrogen RNaseOUT (40 U) and Invitrogen M-MLV Reverse Transcriptase (200 U). RT reaction was left at 25°C for 10 min, followed by 42°C incubation for 50 min. The reaction was terminated by heating at 85°C for 5 min. PCR reactions included 1.5 μl of this reaction, 500 nM Cy3 forward and reverse primers, and were incubated at 95°C for 3 min, 35 cycles of (30 s at, 95°C, 30 s at 58°C, 30 s at 72°C), and a final incubation at 72°C for 3 min. Equal volumes of RT–PCR products were combined with 95% formamide/dye mixture and denatured at 95°C for 10 min. This mixture was then loaded onto a 5% denaturing acrylamide gel (1× TBE). Gels were dried prior to scanning on a Molecular Imager FX System. Poly(A) enrichment of total RNAs was performed using the Ambion poly(A) purist MAG kits as described (12).

Amplification of cleavage products and sequencing analysis

For the adaptor ligation of cleavage products carrying 5′-phosphate groups, an adaptor RNA was purchased from Dharmacon. Total RNAs from various strains were ligated with the adaptor RNA on their 5′-phosphate ends, reverse transcribed using the E3 REV primer, and amplified by PCR. The primer pair for the PCR consisted of a primer that was the DNA version of the adaptor sequence, and the E3 Rev primer.

RESULTS

Accumulation of *MAT*a1 transcripts in *rnt1Δ* cells

Previous microarray analysis of the transcriptome of cells lacking the double-stranded RNA endonuclease Rnt1p revealed that Rnt1p triggers the degradation of mRNAs involved in iron uptake and homeostasis as well as two unspliced pre-mRNAs, *RPS22B* and *RPL18A* (16,19). To investigate if Rnt1p targets additional unspliced precursors for degradation, we mined these microarrays to search for additional intron-containing transcripts which would be subject to Rnt1p-mediated degradation. Such transcripts are more abundant in cells lacking Rnt1p activity because the absence of Rnt1p-mediated nuclear degradation of the unspliced pre-mRNA prevents competition with splicing, and increases the pool of RNA substrates directed towards the splicing pathway. These microarrays showed that the *MAT*a1 mRNA was expressed at higher levels in the *rnt1Δ* strain compared to wild-type. In order to confirm the microarray data, we analyzed *MAT*a1 expression in wild-type and *rnt1Δ* cells in both *MAT*a and *MAT*alpha mating types in the SK1 background strain. This strain is frequently used to study events of meiosis and sporulation due to the fast and effective sporulation properties of their diploids (13). Northern analysis showed that the *MAT*a1 mRNA accumulated at least four times more in *rnt1Δ* cells than in wild-type cells (Figure 1B). In the case of *MAT*alpha cells, no *MAT*a1 signal was detected for either wild-type or *rnt1Δ* cells, which showed that the accumulation of *MAT*a1 in the *rnt1Δ* strain was not due to a derepression of the silent mating-type locus *HMR*a-1. The *MAT*a1 transcript was also three times more abundant in the diploid *rnt1ΔΔ* strain than in the isogenic wild-type diploid cells or heterozygous strains (Figure 1B). Agarose northern blots, such as the ones shown in Figure 1 were not able to separate unspliced precursors from spliced mRNAs, because of the small size of *MAT*a1 introns. As shown below, the accumulating *MAT*a1 in *rnt1Δ* cells seemed to result from at least two separate products, one being the mature mRNA, and the other possibly the unspliced, or a partially spliced versions of the transcript.

Rnt1p cleaves a non-canonical stem–loop structure that encompasses the 5′-splice site of intron2

The previous experiments suggested that Rnt1p might cleave the *MAT*a1 precursor transcript to eliminate unspliced species. To further test this hypothesis we generated an *in vitro* transcript containing the *MAT*a1 exons and introns, and incubated it with recombinant Rnt1p or with buffer alone. We found two major cleavage sites for Rnt1p in this model *MAT*a1 transcript (Figure 1C). The first one (#1, Figure 1C) did not match to any specific structure. However, the second major site

(#2, Figure 1C) corresponded to a sequence on a predicted stem–loop structure, which bridges the second exon and the second intron and contains the 5′-splice site of the second intron (Figure 1D). The location of this cleavage site fits well with the properties of Rnt1p, which has been shown to cleave 14- to 16-bp away from terminal loops (20). However, the terminal loop found in this predicted structure is not a canonical AGNN tetraloop, which Rnt1p has been shown to bind and recognize (20,21). Instead, a 7-nt loop containing the AGNN motif is present (Figure 1D).

To detect a corresponding Rnt1p cleavage product *in vivo*, we used a linker-mediated RT–PCR technique, which allows the detection of RNase III cleavage products by taking advantage of the 5′-phosphate groups generated by RNase III cleavage, a strategy similar to the RNA adapter ligation methods used in 5′-RACE and miRNA cloning kits (Ambion). These cleavage products are normally unstable because they are rapidly degraded but inactivation of the Xrn1p and Rat1p 5′–3′ exonucleases allows their detection (14,16,18). Using this technique, we detected small amounts of a specific product in wild-type cells, the abundance of which was largely increased in an *xrn1Δrat1-1*strain (Figure 1E). This product was completely undetectable in samples extracted from a *rnt1Δ* strain, further suggesting that it corresponds to a Rnt1p cleavage product. Precise sizing analysis of this product showed that the adaptor was ligated to a sequence corresponding to the 3′-side of the predicted stem–loop (Figure 1D; *in vivo* arrow). This sequence was found to be directly opposite to the site where the cleavage product was detected *in vitro* (Figure 1C). Thus, the *in vitro* cleavage and *in vivo* mapping experiments results fit well to demonstrate that Rnt1p cleaves a structure within the *MAT*a1 transcript that bridges the second exon and the second intron.

Accumulation of *MAT*a1 transcripts in nuclear RNA degradation mutants

Previous studies had shown that degradation of unspliced species of *RPS22B* relies on Rnt1p, but also on the action of the 5′–3′ exonucleases Xrn1p and Rat1p (16). To further investigate the mechanisms of degradation of *MAT*a1 transcripts, we analyzed its expression in a panel of RNA degradation mutants. This included the *rat1-1* strain, in which Rat1p is inactivated using a thermosensitive allele (14), the *xrn1Δ* strain, which carries a deletion of the gene encoding the cytoplasmic Xrn1p exonuclease, and the *rrp6Δ* strain containing a deletion of the nuclear exosome component Rrp6p. The *rnt1Δ* strain was included for comparison. We also analyzed *MAT*a1 levels in a combination of double or triple mutant strains (Figure 2). Northern analysis of *MAT*a1 expression in the *xrn1Δ rat1-1* strain showed an increase of *MAT*a1 transcripts at permissive temperature (Figure 2A), which was slightly lower than the accumulation observed in the *rnt1Δ* strain. However when this strain was combined with the *rnt1Δ* deletion, we observed a dramatic accumulation of signal in the amount of *MAT*a1 transcripts. Interestingly, we also observed a large increase of *MAT*a1 signal in the *rnt1Δrrp6Δ* strain at 25°C, as well as in the triple mutant combining the *rrp6Δ* deletion to the *xrn1Δ rat1-1* strain. The RNA species detected for *MAT*a1 in the *xrn1Δ* strain migrate slightly faster than those detected in the other strains, possibly because they correspond to deadenylated forms.

When these strains were shifted to 37°C, we observed a very strong accumulation of *MAT*a1 transcripts in the *xrn1Δ rat1-1* strain, which was comparable to that observed in the *rnt1Δ* strain grown in the same conditions. We also observed an increase of signal in the *rnt1Δ* strain compared to 25°C. The combination of these mutants with other mutations did not result in an increase of signal, suggesting that Rnt1p and Rat1p play a major role in the degradation of *MAT*a1 transcripts when these strains are shifted to 37°C. Because of the small size of *MAT*a1 introns, the poor resolution of spliced and unspliced species in agarose northern blots prevented us from concluding whether the mature *MAT*a1 or unspliced species are the predominant species accumulating in RNA degradation mutants, or if an accumulation of both contribute to the large increase of signal. To investigate if unspliced *MAT*a1 transcripts contribute to the increase of signal observed in Figure 2A for the different mutant strains, we tried to hybridize membranes with probes specific to intronic sequences. This proved to be challenging, since the small size of each *MAT*a1 intron (54 and 52 nt) made the use of riboprobes or random primed probes impractical. In addition the low complexity of *MAT*a1 intronic sequences made it difficult to design oligonucleotide probes. However one sequence in intron2 allowed us to detect unspliced and/or partially spliced species of *MAT*a1 containing intron2 (Figure 2B). This probe detected the accumulation of unspliced species in the *rnt1Δ* strain at 25°C, which was further increased in the *xrn1Δ rat1-1rnt1Δ* triple mutant strain. When shifted to 37°C, we also observed a stronger intronic signal in the *rnt1Δ* strain, and in the *xrn1Δ rat1-1* strain and in its derivatives (Figure 2B). This result suggested that Rnt1p, as well as Rat1p contribute to degrading unspliced species of *MAT*a1. Based on the comparison of the patterns observed in Figure 2A and B, it is likely that the large increase in signal observed for the various degradation mutants is the result of an increase in both unspliced and spliced species of *MAT*a1.

Analysis of *MAT*a1 expression by RT–PCR confirms the accumulation of unspliced forms of *MAT*a1 in Rnt1p and Rat1p-deficient cells

The previous data suggested that cleavage of the *MAT*a1 pre-mRNA transcript by Rnt1p would initiate degradation of unspliced or partially spliced transcripts that still retain intron2, and also revealed a role for nuclear degradation by Rat1p and the nuclear exosome in eliminating these species. However, it was difficult to fully characterize the different RNAs accumulating in the various strains by northern blot because of their relatively low abundance, their poor resolution and the difficulty to use intron specific probes. To circumvent these

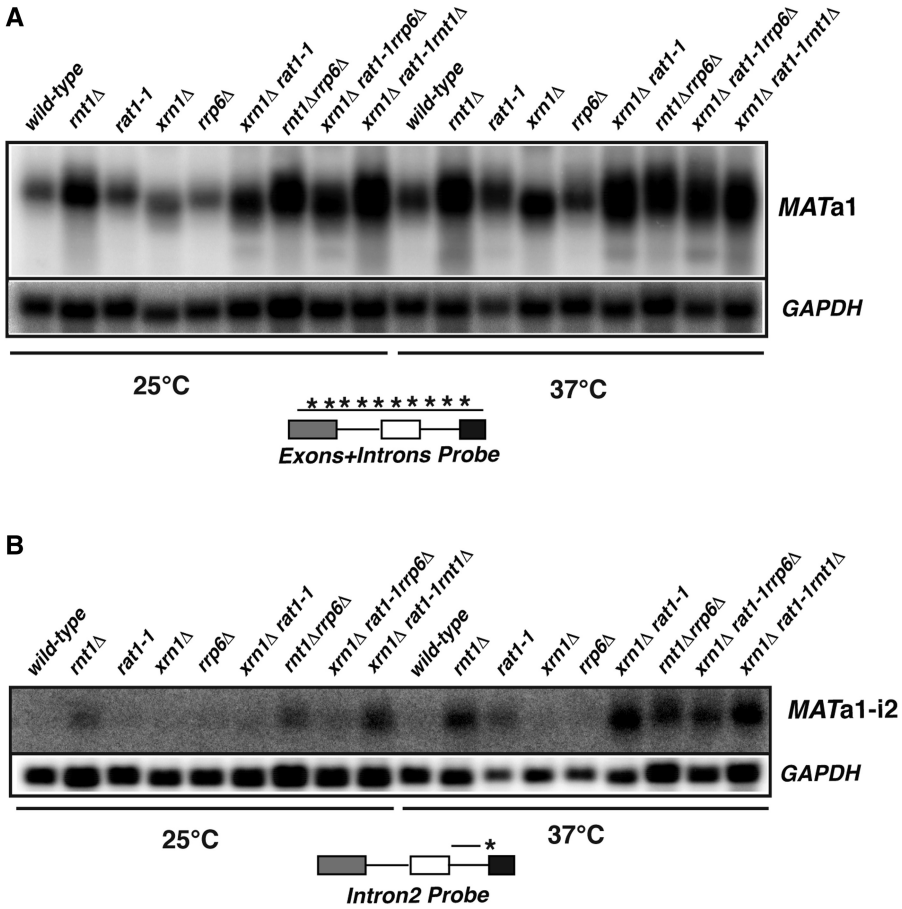

Figure 2. Northern blot analysis of *MAT*a1 expression in *rnt1Δ* and exonuclease mutant strains. The isozymes of the Glyceraldehyde 3 Phosphate Dehydrogenase enzyme (G3PDH, or GAPDH) were used as a loading control. (**A**) The membrane was hybridized with a riboprobe covering most of the *MAT*a1 sequence (3 exons and 2 introns) prior to GAPDH hybridization. **(B)** The membrane was hybridized with an intron2-specific oligonucleotide probe (Supplementary Table S1).

problems, we analyzed *MAT*a1 expression in all strains by RT–PCR (Figure 3A). This analysis confirmed the accumulation of fully unspliced and partially spliced transcripts still retaining intron 2 in the *rnt1Δ* strain (Figure 3A). We did not observe by RT–PCR the higher levels of spliced *MAT*a1 mRNAs in the *rnt1Δ* strain detected by northern blots in Figures 1 and 2. We hypothesized that the number of PCR cycles used to detect unspliced species led to a saturation of the signal for the spliced mRNA in these experiments. Using a smaller number of PCR cycles, we were able to confirm higher levels of spliced mRNAs in the *rnt1Δ* strain compared to the wild-type (Figure S1). In addition, we also detected the higher abundance of the spliced mRNAs in the *rnt1Δ* strain by primer extension analysis using an exon3 specific primer (Figure 3B). Collectively, these results confirm the higher accumulation of spliced *MAT*a1 mRNAs in the *rnt1Δ* strain and show that Rnt1p cleavage competes with splicing, explaining the increased abundance of spliced *MAT*a1 in the absence of Rnt1p.

This technique also allowed us to investigate which exonucleases contribute to the degradation of the unspliced or partially spliced *MAT*a1 transcripts. The largest effect was observed upon inactivation of the nuclear exosome at 25°C, and of Rat1p in the *rat1-1* strain or in the *xrn1Δ rat1-1* strain at 37°C. The two species that accumulate specifically upon a shift to non-permissive temperature in the *xrn1Δ rat1-1* strain could also be detected by primer extension analysis using an exon3 (Figure 3B) or an intron2 specific primer (Figure 3C), suggesting that they corresponded to fully unspliced and partially spliced species still containing intron2. Sequencing of the RT–PCR products confirmed the identity of these species (data not shown). No accumulation of unspliced or partially spliced species was observed upon inactivation of Xrn1p (Figure 3A) or of Upf1p (Figure S2A), showing that in contrast to many yeast pre-mRNAs (17), unspliced and partially spliced species of *MAT*a1 are not targeted by nonsense-mediated decay (NMD). In addition, inactivation of Xrn1p in the *rat1-1* strain did not result in a major increase of unspliced pre-mRNAs compared to the *rat1-1* stain alone, showing that Rat1p is primarily responsible for the degradation of unspliced and partially spliced *MAT*a1 transcripts. We also found that inactivation of the nuclear exosome in the *rnt1Δ* strain led to an increase of unspliced pre-mRNA, showing that the nuclear exosome can cooperate with Rnt1p in discarding unspliced or incompletely spliced *MAT*a1 species. Overall

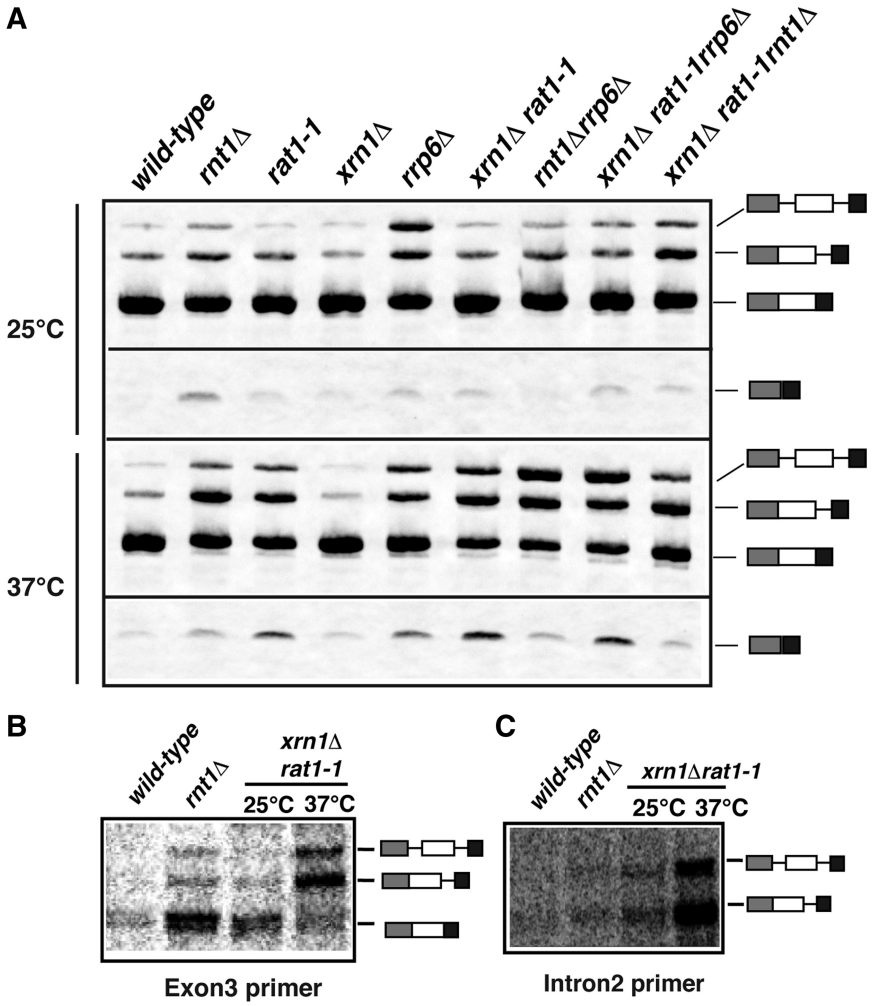

Figure 3. RT–PCR and primer extension analysis of *MAT*a1 expression in *rnt1Δ* and ribonuclease mutant strains. **(A)** RT–PCR analysis. All panels show RT–PCR products obtained using a Cy3-labeled exon1 primer and an unlabeled exon3-primer specific for *MAT*a1 in the corresponding strains grown at the indicated temperatures. The exon2-skipped products (shown on the bottom panels) were detected on the same gel as the spliced and unspliced species but that portion of the gel was scanned separately to increase the signal to noise ratio. No other species were detected in the portions of the gel that are not shown. **(B)** Primer extension analysis of *MAT*a1 in the corresponding strains using an oligonucleotide hybridizing to exon3. **(C)** Primer extension analysis of *MAT*a1 in the corresponding strains using an oligonucleotide hybridizing to intron2.

these results show that at least three different nuclear RNA degradation systems can affect unspliced or incompletely spliced *MAT*a1 transcripts: Rnt1p, Rat1p and the nuclear exosome.

Exon2-skipped species of *MAT*a1 and of other genes containing two introns accumulate in the *rat1-1* and *rrp6Δ* strains

Using the RT–PCR approach described above, we detected a new short molecular weight species migrating faster than fully spliced mRNA, which accumulated specifically in nuclear RNA degradation mutants (Figure 3A, bottom panels). This species accumulated most abundantly at 25°C in the *rnt1Δ* strain (Figure 3A and Supplementary Figure S1A). When shifted to 37°C, this species was found predominantly in the *rat1-1* strain, and in the *rrp6Δ* strain, or in double or triple mutants in which Rat1p is inactivated (Figure 3A). Sequencing of this product (not shown) revealed that it corresponds to a spliced mRNA in which exon 2 was skipped and where exon 1 was spliced directly to exon 3. This result suggested that these exon2-skipped species are preferentially targeted for degradation by nuclear exonucleases. We did not detect any accumulation of the exon skipped species in a strain carrying a single deletion of *XRN1*, or in the *upf1Δ* strain (Supplementary Figure S2A), showing that it is not subjected to nonsense-mediated mRNA decay, despite its lack of extended open-reading frame.

The accumulation of the exon2-skipped species in the *rnt1Δ* strain at 25°C is unlikely to reflect a direct degradation function for Rnt1p, since the predicted target stem–loop structure is absent in this product. To further test this hypothesis, we overexpressed Rnt1p or a catalytically inactive mutant derivative in the *rat1-1* strain in order to investigate whether Rnt1p overexpression could decrease the levels of the exon2-skipped species that accumulate in the absence of Rat1p activity. The results shown in

Supplementary Figure S3 show that overexpression of Rnt1p does not change the accumulation of exon2-skipped species in the context of the *rat1-1* strain. Thus, it is unlikely that Rnt1p directly cleaves these species. Rather, we favor a model in which Rnt1p cleavage decreases the fraction of precursors that can fold in a conformation that favors the skipping of exon2 (see 'Discussion' section).

Rat1p has been shown to promote transcription termination of RNA polymerase II, both in downstream regions (22) and within the body of genes (23). Association of Rat1p with Rai1p promotes this function, and strains lacking Rai1p are also deficient in transcription termination (22). To investigate if accumulation of the exon2-skipped species in the *rat1-1* strain is an indirect consequence of a transcription termination defect, we assessed exon2-skipped species levels in *rai1Δ* cells. In contrast to the *rat1-1* control, we were unable to detect any accumulation of the exon2-skipped species in samples extracted from the *rai1Δ* strain (Supplementary Figure S2B). We conclude that the accumulation of exon2-skipped species is unlikely to result from indirect transcription termination defects, but more likely to a lack of degradation by Rat1p.

To further characterize why unspliced and exon2 skipped species are preferentially targeted by Rat1p, we investigated whether a lack of polyadenylation would potentially impair their export to the cytoplasm, making them more susceptible to degradation by this nuclear exonuclease. We purified the polyadenylated fraction of RNAs from yeast total RNAs using oligo-dT affinity, and analyzed the enrichment of the different *MAT*a1 transcripts in the poly(A)+ fractions (Supplementary Figure S2C). Interestingly, both the various unspliced species and the exon2-skipped species were found in the poly(A)+ fractions of the *rat1-1* strain, suggesting that these species are correctly polyadenylated. This result suggests that a lack of polyadenylation is not the reason why these species are preferentially targeted by Rat1p.

The previous data showed that Rat1p and the nuclear exosome degrade transcripts resulting from mis-splicing events in which the spliceosome had skipped the central exon of *MAT*a1. To investigate if this effect is specific to *MAT*a1 or can be extended to other genes, we analyzed the expression of other genes containing two introns (*DYN2*, *SUS1*, *YOS1*) in the *rat1-1* and *rrp6Δ* strains by RT–PCR. First, we found various unspliced species accumulating in the *rat1-1* and *rrp6Δ* strains (Figure 4), showing that these unspliced RNAs are degraded by Rat1p and the nuclear exosome, as shown above for *MAT*a1 and in previous studies for other intron containing genes (24). Figure 4 also shows that an increase of exon2-skipped species of *SUS1*, *YOS1* and *DYN2* could be detected at permissive temperature (25°C) in the *rrp6Δ* strain. After a shift to 37°C, we also observed a higher accumulation of these exon-skipped species in the *rat1-1* and *rrp6Δ* strains. These results show that exon2-skipped species of several genes accumulate to higher levels when the activity of nuclear exonucleases is disrupted, suggesting that the degradation of these exon skipped species is under the control of nuclear RNA surveillance.

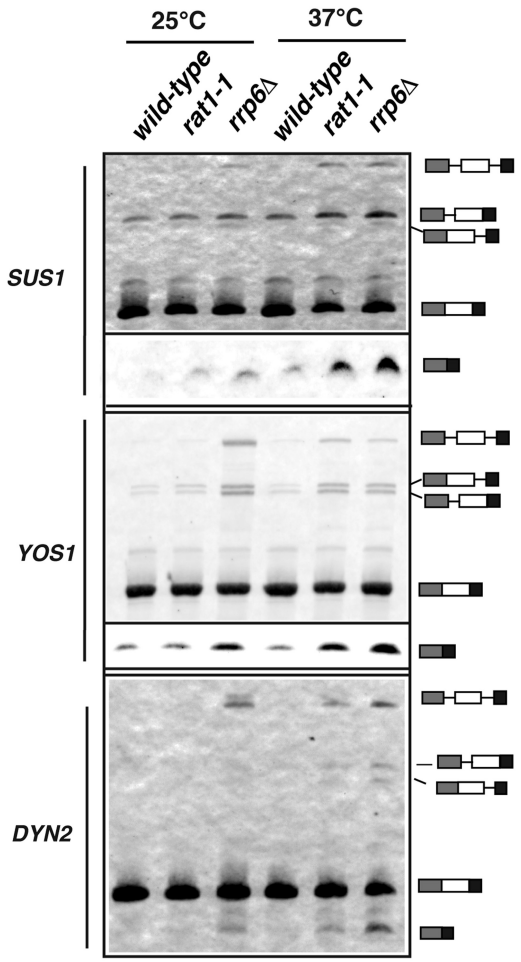

Figure 4. Analysis of exon2 skipping for the *DYN2*, *SUS1* and *YOS1* genes in the *rat1-1* and *rrp6Δ* strains. All panels show RT–PCR products obtained using a Cy3-labeled exon1 primer and an unlabeled exon3-primer specific for the corresponding genes in the strains grown at the indicated temperatures. The exon2-skipped products (shown on the bottom panels) were detected on the same gels as the spliced and unspliced species but that portion of the gel was scanned separately to increase the signal to noise ratio. No other species were detected in the portions of the gel that are not shown.

DISCUSSION

In this study, we used a genetic analysis to investigate the mechanisms of degradation that target the different RNAs produced by the *MAT*a1 gene. We found that the unspliced pre-mRNA, as well as a partially spliced version of *MAT*a1 that retains intron2 are degraded by Rnt1p, Rat1p and by the nuclear exosome (Figure 3A). As shown previously for the *RPS22B* gene (16), Rnt1p cleavage probably competes with splicing of the pre-mRNA, which explains the increase of abundance of the *MAT*a1 mRNA in strains lacking Rnt1p (Figures 1 and 2; Supplementary Figure S1). We note that the terminal loop of the stem–loop structure cleaved by Rnt1p might not be optimal, since it contains the AGNN motif but is a 7-nt loop (Figure 1D) instead of the canonical tetraloop motif (20,25). This suboptimal structure might explain why Rat1p is the major

degradative activity that targets unspliced *MAT*a1 pre-mRNAs, rather than Rnt1p.

We have postulated that the increased abundance of unspliced and partially spliced species in RNA degradation mutants reflect their stabilization. Because these species do not accumulate to significant levels in wild-type cells, we were unable to compare their turnover rates and to estimate their stability in the different backgrounds. Thus, we cannot formally rule out the possibility that the splicing efficiency of *MAT*a1 is influenced by the disruption of degradative activities. For example, it was shown recently that RNA degradation complexes can modulate the rate of other steps in gene expression such as transcriptional elongation (26), and the rate of elongation might affect splicing efficiency. While we cannot formally exclude the possibility of indirect effect for exonuclease mutants, the observation that spliced *MAT*a1 mRNA levels increase in the absence of Rnt1p is consistent with a direct role for Rnt1p in cleaving unspliced mRNAs and a model suggesting that Rnt1p cleavage competes with splicing of the pre-mRNA (Figure 5A).

As opposed to many yeast pre-mRNAs (17), unspliced *MAT*a1 transcripts are not subject to nonsense-mediated mRNA decay (Supplementary Figure S2A), but rely mostly on nuclear degradation pathways. It is possible that these species are not exported very fast, and thus rely mostly on nuclear degradation, as described previously for other genes (24) and for the *DYN2*, *SUS1* and *YOS1* genes (Figure 4). Regardless of the reason why *MAT*a1 seem to rely on nuclear degradation, our results show that the splicing of *MAT*a1 might be suboptimal. This relative inefficient splicing might be caused by the small size of its introns (~50 nt), which are smaller than most *S. cerevisiae* introns. In addition, folding of the stem–loop structure that sequesters the 5′-splice site of intron2 and prevents U1 snRNP binding (Figure 5A) might also explain the inefficiency of intron2 splicing and why species containing this intron are detected in ribonuclease mutants. Thus, nuclear degradation mechanisms have been selected to limit the accumulation of mRNAs that have escaped the splicing machinery, and also to prevent their expression in the cytoplasm as unfunctional proteins.

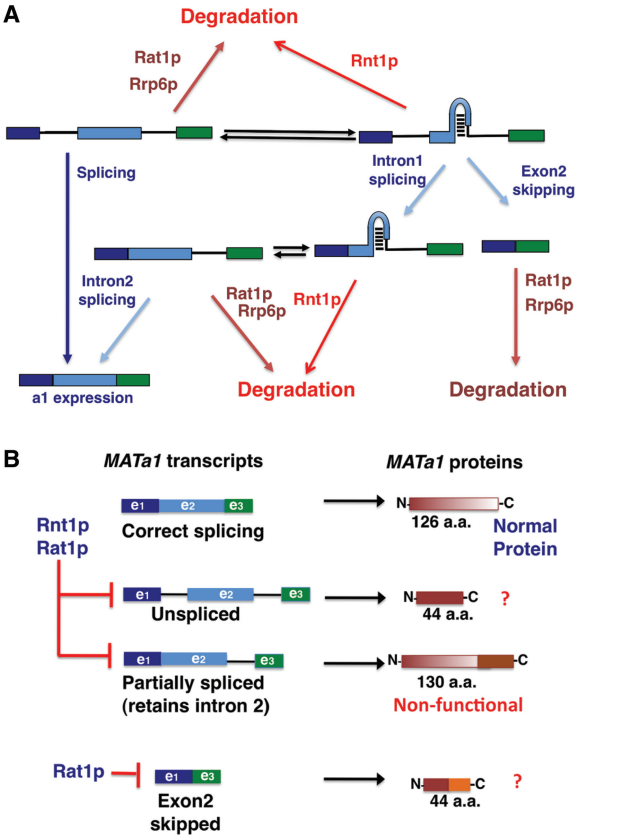

Figure 5. Nuclear RNA quality control discards incompletely or aberrantly spliced forms of *MAT*a1 that result in aberrant a1 isoforms. **(A)** Model of degradation of unspliced, partially spliced and mis-spliced forms of *MAT*a1 by Rnt1p, Rat1p and the nuclear exosome. **(B)** Diagram of the different isoforms of a1 encoded by the different unspliced, partially spliced and mis-spliced forms of *MAT*a1.

Role of the partially spliced *MAT*a1 pre-mRNA encoding a1′

In contrast to most intron containing genes, some partially spliced species of *MAT*a1 encode proteins that do not correspond to truncated forms of the normal protein (Figure 5B). The partially spliced *MAT*a1 mRNA species that accumulates in Rnt1p and Rat1p-deficient strains had been previously analyzed in splicing mutants (9) and further studied by Ner and Smith (8) via experiments on branch point mutants. In this study, it was first tested whether the protein encoded by the *MAT*a1 transcript including Intron2 (termed a1′) could have a biological role and work together with mature a1. This partially spliced transcript would encode a protein that is different and longer than mature a1, especially in the C-terminal domain (Figure 5). The C-terminal domain of a1 is where DNA-binding occurs through Helix 3 when in complex with alpha2. Interactions with alpha2 occur between Helices 1 and 2 and are unaffected in a1′ based on primary sequence and structural analysis (27) (PDB code: 1F43). Specific residues on a1 that are important for contacting DNA are five residues within Helix 3 (4). In their study, Ner and Smith suggested that the a1′ protein does not have any biological role, as it is unable to rescue a1 deficiency (8). However this protein might potentially act as a dominant negative inhibitor, explaining the requirement to limit its accumulation through the degradation of the mRNA encoding this isoform.

Although constitutively expressed in cells of the ‘a’ mating-type as a part of the haploid *MAT*a transcriptional program, the a1 protein has not yet been characterized to have a direct function in these cells (28,29). In diploid cells, this protein combines with the alpha2 protein in order to repress haploid-specific gene expression. In this study, we have assessed the role of Rat1p and Rnt1p in regulation of the *MAT*a1 transcript in haploid cells. Rnt1p is already known to have important roles in cell-cycle regulation and cell division (30), and is a crucial enzyme for correct processing of numerous non-coding RNAs as well as degradation of mRNAs. Our microarray data

show that one of the genes that are considerably down-regulated (−12.3-fold) in *rnt1Δ* cells encodes HO, the mating-type switching endonuclease gene that is known to be repressed in diploids by the a1 and alpha2 heterodimer (31,32). Considering the accumulation of mature *MAT*a1 in *rnt1Δ* strains, as well as partially unspliced forms, one hypothesis is that the excess of a1 could associate with the a2 protein, which has many sequence similarities to alpha2, to act in repressing HO even within haploid cells. Further experiments are required to prove this model.

A novel RNA surveillance mechanism to degrade exon-skipped species

Strikingly, we also found that incorrectly spliced mRNAs are generated from the *MAT*a1 locus, in which the exon2 is skipped and exon1 is spliced to exon3. These species are preferentially degraded by Rat1p and the nuclear exosome, but they also accumulate in the absence of Rnt1p. This suggests that formation of the target stem–loop structure that bridges exon2 and intron2 favors exon2 skipping for the transcripts that have folded in this structure (Figure 5A). Formation of this structure would sequester the 5′-splice site of intron2 from U1 snRNP binding, promoting a direct splicing of exon1 to exon3 (Figures 1D and 5A). Thus the increase of exon-skipped species in the *rnt1Δ* strain (Figure 3A and Supplementary Figure S1A) might not be due to the fact that Rnt1p directly contributes to degrading exon skipped species, but rather because it eliminates a fraction of the pre-mRNAs which have folded in a manner that promotes the skipping of exon 2 (Figure 5A). In contrast, our data suggest that Rat1p and the nuclear exosome are directly responsible for degrading these exon-skipped species. Strikingly, we found that exon2-skipped species of other genes that contain two introns also accumulate when Rat1p or the nuclear exosome are inactivated (Figure 4). This suggests that nuclear RNA degradation plays a general role in degrading species that have been incorrectly spliced. This type of event is favored by the small size of central exons in yeast, facilitating the recognition of the downstream 3′-splice site in intron2, rather than the correct 3′-splice site of intron1.

We presumed that the increased abundance of the exon2-skipped products when Rat1p or the nuclear exosome are inactivated reflects their stabilization. However, we cannot formally exclude the possibility that inactivation of Rat1p or of the nuclear exosome indirectly affects splicing, and that this change of splicing efficiency is responsible for an increased rate of exon skipping. For instance, the accumulation of this product might reflect functions for Rat1p other than direct degradation, such as promoting transcriptional termination within coding regions (23). Inactivation of Rat1p results in a faster RNA polymerase, and it is known that a faster rate of elongation promotes exon skipping as shown in mammalian cells. However, *RAI1*-deficient cells that are also deficient in termination (22) do not exhibit an accumulation of the exon2-skipped species. This suggests that accumulation of the exon2-skipped species is likely due to its lack of degradation.

It remains to be understood why these exon-skipped species are preferentially targeted by Rat1p or the nuclear exosome in the nucleus, and not by nonsense-mediated decay. Since Rat1p associates co-transcriptionally with the RNA polymerase (22), it is possible that it acts non-discriminately on non-capped RNAs, and that exon-skipped species are particularly prone to Rat1p-mediated degradation. Inactivation of Xrn1p, the general cytoplasmic exonuclease involved in NMD does not increase the amount of exon2 skipped species, even when Rat1p is inactivated (Figure 3A). This suggests that these exon2 skipped species are not exported to the cytoplasm but are retained in the nucleus. This would explain why these exon-skipped species are also affected by the nuclear exosome. Regardless of the precise mechanism of nuclear retention, the finding that this nuclear RNA degradation pathway targets species that are incorrectly spliced underscores the importance of nuclear RNA surveillance in the quality control of gene expression and identify a novel mechanism of RNA surveillance for incorrect splicing.

SUPPLEMENTARY DATA

Supplementary Data are available at NAR Online: Supplementary Table 1, Supplementary Figures 1–3.

ACKNOWLEDGEMENTS

The authors thank members of the Chanfreau laboratory, Al Courey and H. Madhani for helpful discussions.

FUNDING

NIGMS (grant GM61518); USPHS National Research Service Award GM07104 to T.K. Funding for open access charge: NIGMS (grant GM61518 and GM07104).

Conflict of interest statement. None declared.

REFERENCES

1. Mathias,J.R., Hanlon,S.E., O'Flanagan,R.A., Sengupta,A.M. and Vershon,A.K. (2004) Repression of the yeast HO gene by the MATalpha2 and MATa1 homeodomain proteins. *Nucleic Acids Res.*, **32**, 6469–6478.
2. Johnson,A.D. (1995) Molecular mechanisms of cell-type determination in budding yeast. *Curr. Opin. Genet. Dev.*, **5**, 552–558.
3. Goutte,C. and Johnson,A.D. (1988) a1 protein alters the DNA binding specificity of alpha 2 repressor. *Cell*, **52**, 875–882.
4. Li,T., Stark,M.R., Johnson,A.D. and Wolberger,C. (1995) Crystal structure of the MATa1/MAT alpha 2 homeodomain heterodimer bound to DNA. *Science*, **270**, 262–269.
5. Goutte,C. and Johnson,A.D. (1993) Yeast a1 and alpha 2 homeodomain proteins form a DNA-binding activity with properties distinct from those of either protein. *J. Mol. Biol.*, **233**, 359–371.
6. Phillips,C.L., Stark,M.R., Johnson,A.D. and Dahlquist,F.W. (1994) Heterodimerization of the yeast homeodomain transcriptional regulators alpha 2 and a1 induces an interfacial helix in alpha 2. *Biochemistry*, **33**, 9294–9302.

7. Kohrer,K. and Domdey,H. (1988) Splicing and spliceosome formation of the yeast MATa1 transcript require a minimum distance from the 5′ splice site to the internal branch acceptor site. *Nucleic Acids Res.*, **16**, 9457–9475.
8. Ner,S.S. and Smith,M. (1989) Role of intron splicing in the function of the MATa1 gene of Saccharomyces cerevisiae. *Mol. Cell. Biol.*, **9**, 4613–4620.
9. Miller,A.M. (1984) The yeast MATa1 gene contains two introns. *EMBO J.*, **3**, 1061–1065.
10. Baudin,A., Ozier-Kalogeropoulos,O., Denouel,A., Lacroute,F. and Cullin,C. (1993) A simple and efficient method for direct gene deletion in Saccharomyces cerevisiae. *Nucleic Acids Res.*, **21**, 3329–3330.
11. Chanfreau,G., Rotondo,G., Legrain,P. and Jacquier,A. (1998) Processing of a dicistronic small nucleolar RNA precursor by the RNA endonuclease Rnt1. *EMBO J.*, **17**, 3726–3737.
12. Egecioglu,D.E., Henras,A.K. and Chanfreau,G.F. (2006) Contributions of Trf4p- and Trf5p-dependent polyadenylation to the processing and degradative functions of the yeast nuclear exosome. *RNA*, **12**, 26–32.
13. Chu,S., DeRisi,J., Eisen,M., Mulholland,J., Botstein,D., Brown,P.O. and Herskowitz,I. (1998) The transcriptional program of sporulation in budding yeast. *Science*, **282**, 699–705.
14. Petfalski,E., Dandekar,T., Henry,Y. and Tollervey,D. (1998) Processing of the precursors to small nucleolar RNAs and rRNAs requires common components. *Mol. Cell. Biol.*, **18**, 1181–1189.
15. Longtine,M.S., McKenzie,A. 3rd, Demarini,D.J., Shah,N.G., Wach,A., Brachat,A., Philippsen,P. and Pringle,J.R. (1998) Additional modules for versatile and economical PCR-based gene deletion and modification in Saccharomyces cerevisiae. *Yeast*, **14**, 953–961.
16. Danin-Kreiselman,M., Lee,C.Y. and Chanfreau,G. (2003) RNAse III-mediated degradation of unspliced pre-mRNAs and lariat introns. *Mol. Cell.*, **11**, 1279–1289.
17. Sayani,S., Janis,M., Lee,C.Y., Toesca,I. and Chanfreau,G.F. (2008) Widespread impact of nonsense-mediated mRNA decay on the yeast intronome. *Mol. Cell.*, **31**, 360–370.
18. Lee,C.Y., Lee,A. and Chanfreau,G. (2003) The roles of endonucleolytic cleavage and exonucleolytic digestion in the 5′-end processing of S. cerevisiae box C/D snoRNAs. *RNA*, **9**, 1362–1370.
19. Lee,A., Henras,A.K. and Chanfreau,G. (2005) Multiple RNA surveillance pathways limit aberrant expression of iron uptake mRNAs and prevent iron toxicity in S. cerevisiae. *Mol. Cell.*, **19**, 39–51.
20. Chanfreau,G., Buckle,M. and Jacquier,A. (2000) Recognition of a conserved class of RNA tetraloops by Saccharomyces cerevisiae RNase III. *Proc. Natl Acad. Sci. USA*, **97**, 3142–3147.
21. Wu,H., Henras,A., Chanfreau,G. and Feigon,J. (2004) Structural basis for recognition of the AGNN tetraloop RNA fold by the double-stranded RNA-binding domain of Rnt1p RNase III. *Proc. Natl Acad. Sci. USA*, **101**, 8307–8312.
22. Kim,M., Krogan,N.J., Vasiljeva,L., Rando,O.J., Nedea,E., Greenblatt,J.F. and Buratowski,S. (2004) The yeast Rat1 exonuclease promotes transcription termination by RNA polymerase II. *Nature*, **432**, 517–522.
23. Jimeno-Gonzalez,S., Haaning,L.L., Malagon,F. and Jensen,T.H. (2010) The yeast 5′-3′ exonuclease Rat1p functions during transcription elongation by RNA polymerase II. *Mol. Cell.*, **37**, 580–587.
24. Bousquet-Antonelli,C., Presutti,C. and Tollervey,D. (2000) Identification of a regulated pathway for nuclear pre-mRNA turnover. *Cell*, **102**, 765–775.
25. Wu,H., Yang,P.K., Butcher,S.E., Kang,S., Chanfreau,G. and Feigon,J. (2001) A novel family of RNA tetraloop structure forms the recognition site for Saccharomyces cerevisiae RNase III. *EMBO J.*, **20**, 7240–7249.
26. Kruk,J.A., Dutta,A., Fu,J., Gilmour,D.S. and Reese,J.C. (2011) The multifunctional Ccr4-Not complex directly promotes transcription elongation. *Genes Dev.*, **25**, 581–593.
27. Anderson,J.S., Forman,M.D., Modleski,S., Dahlquist,F.W. and Baxter,S.M. (2000) Cooperative ordering in homeodomain-DNA recognition: solution structure and dynamics of the MATa1 homeodomain. *Biochemistry*, **39**, 10045–10054.
28. Haber,J.E. (1998) Mating-type gene switching in Saccharomyces cerevisiae. *Annu. Rev. Genet.*, **32**, 561–599.
29. Zill,O.A. and Rine,J. (2008) Interspecies variation reveals a conserved repressor of alpha-specific genes in Saccharomyces yeasts. *Genes Dev.*, **22**, 1704–1716.
30. Catala,M., Lamontagne,B., Larose,S., Ghazal,G. and Elela,S.A. (2004) Cell cycle-dependent nuclear localization of yeast RNase III is required for efficient cell division. *Mol. Biol. Cell.*, **15**, 3015–3030.
31. Sprague,G.F. Jr (1991) Signal transduction in yeast mating: receptors, transcription factors, and the kinase connection. *Trends Genet.*, **7**, 393–398.
32. Roberts,C.J., Nelson,B., Marton,M.J., Stoughton,R., Meyer,M.R., Bennett,H.A., He,Y.D., Dai,H., Walker,W.L., Hughes,T.R. *et al.* (2000) Signaling and circuitry of multiple MAPK pathways revealed by a matrix of global gene expression profiles. *Science*, **287**, 873–880.